COMPUTATIONAL/EXPERIMENTAL STUDIES OF ISOLATED, SINGLE COMPONENT DROPLET COMBUSTION

N93-20213

Frederick L. Dryer
Department of Mechanical and Aerospace Engineering
Princeton University
Princeton, New Jersey 08544-5263

Introduction

Isolated droplet combustion processes have been the subject of extensive experimental and theoretical investigations for nearly 40 years. The gross features of droplet burning are qualitatively embodied by simple theories and are relatively well understood (e.g. ref.1). However, there remain significant aspects of droplet burning, particularly its dynamics, for which additional basic knowledge is needed for thorough interpretations and quantitative explanations of transient phenomena. Spherically-symmetric droplet combustion, which can only be approximated under conditions of both low Reynolds and Grashof numbers, represents the simplest geometrical configuration in which to study the coupled chemical/transport processes inherent within non-premixed flames. Microgravity droplet combustion can closely approximate these conditions, while also giving insights as to how coupling of the above processes is affected by the absence of gravitational forces. Advances in both asymptotic and numerical computational abilities allow more recent analyses of droplet burning to include considerably refined descriptions of the transport and chemical effects, particularly if the spherically symmetric assumption can be maintained. While such improvements in theory represent significant promise for future advances, experimental data available for comparison with theory, without corrections for convective effects, remain relatively limited.

The research summarized here, concerns recent results on isolated, single component, droplet combustion under microgravity conditions, a program pursued jointly with F.A. Williams of the University of California, San Diego. The overall program involves developing and applying experimental methods to study the burning of isolated, single component droplets, in various atmospheres, primarily at atmospheric pressure and below, in both drop towers and aboard space-based platforms such as the Space Shuttle or Space Station (e.g. refs. 2-4). Both computational methods (e.g. ref. 5) and asymptotic methods, the latter pursued mainly at UCSD, (see preceding paper), are used in developing the experimental test matrix, in analyzing results, and for extending theoretical understanding. Methanol, and the normal alkanes, n-heptane, and n-decane, have been selected as test fuels to study time-dependent droplet burning phenomena. The following sections summarize the Princeton efforts on this program, describe work in progress, and briefly delineate future research directions.

Methanol

Methanol is thermophysically, thermochemically, and kinetically, the most well characterized of liquid fuels. Methanol burns diffusively without the production of soot and a number of its combustion intermediates and products, notably water and formaldehyde, are highly soluble in the fuel (refs. 2,7,8). As a result, spherically symmetric modeling of methanol droplet combustion is especially amenable to time-dependent, computational studies which include detailed multi-component transport, thermo-chemistry, and chemical kinetics (ref. 6). Thus, methanol is an ideal fuel selection for providing benchmark comparisons of theory and experiment.

Utilizing the Chemically Reacting Flow Model (CRFM) developed at Princeton (ref. 5), computational studies have been performed including multi-component transport (ref.9), and detailed kinetics (ref. 10). Calculations were compared with experimental data generated in the 2.2 second drop tower (ref. 6) and with ground-based laboratory experiments (refs. 2,8). Droplet gasification rate, flame position, and extinction were shown to be affected by species absorption and dissolution into the liquid phase. The non-linear behavior of the square of the droplet diameter with time and the extinction diameter calculated for the combustion of a methanol droplet in 50% helium/50% oxygen mixtures at atmospheric pressure compare well with 2.2 second drop tower experiments. Calculated flame temperature profiles suggest temperature is an insensitive parameter for experimentally defining flame position. However, experimental measurements of gas phase [OH], and [CH2O] profiles would apparently permit accurate determination of the oxidizer and fuel consumption regions (i.e. flame structure) as well as position.

Additional ground-based experimental and computational work is planned on both pure methanol and methanol-water droplets to further develop fundamental understanding and a space-based test matrix. One-g suspended and free droplet studies have been performed at Princeton on methanol-water mixtures which show interesting effects of initial water content on extinction diameter (refs. 2,7,8). Both 2.2 second and 5 second tower studies are scheduled, pending availability of the NASA-Lewis 2.2 second drop-package and the refurbishment of the 5.0 second tower facility. Computational development of full-flight and ground-test matrices for methanol droplet studies (similar to those described below for n-heptane) require further refinement of the detailed chemistry utilized in the model (ref. 10), particularly its pressure-dependent characteristics. Kinetic model refinements are presently underway, based on other recently published studies (refs. 11-13), and a new variable pressure (1-15 atm.) flow reactor study recently concluded in the author's laboratory (ref. 14). Finally, a reduced mechanism for methanol diffusion flames remains to be developed to assist in parallel asymptotic studies.

Normal Alkanes

Normal-heptane and n-decane have been utilized in many prior droplet burning studies, both in earth's gravitational field (e.g. ref. 15) and in droptowers (e.g. ref. 16). Under microgravity droplet combustion conditions, both exhibit significant soot formation and accumulation (by

thermophoresis) within the surrounding diffusion flame (refs. 17,18). The "sootshell" thus formed and the soot agglomerate densities within it are strongly influenced by ambient pressure, oxygen indices, and diluent species (refs. 2,8), as well as by initial droplet size (ref. 19) and relative gas/droplet convection (refs. 8,18). Associated with the formation and presence of the sootshell, is a reduced droplet gasification rate that can be as much as 40% lower than observed in early drop tower measurements at similar drop sizes (no sootshells present). The burning rate data increase with measured relative gas/droplet convection rate (ref.18), and recent experiments (refs. 2,8) show that, contrary to classical theory, the gasification rate is increased significantly by pressure reduction (through reduced sooting). No fundamental theory has been conclusively established for these effects, but it has been suggested that radiation losses from the sootshell, changes in the temperature-averaged transport properties, and changes in gas-phase volume flux due to soot formation are possible sources of effects which change both the surface gasification rate and flame position (refs. 2,18).

Over some ranges of experimental parameters, droplet disruption and dismemberment is also observed to occur early in the droplet burning history (refs. 8,17,18), while over other ranges of conditions, droplet extinction is observed to occur. Speculations for the mechanisms which produce disruption are: deposition of high-molecular-weight soot precursor intermediates in the liquid phase, resulting in multi-component droplet gasification behavior (ref. 17); collapse of the diffusion flame structure into the soot shell, causing intense disturbances from the soot shell ignition.; soot deposition at the liquid surface; and critical electrostatic charge accumulation in the soot shell and/or droplet surface (refs. 2,8). Recent experiments at one-g suggest that deposition of high molecular weight components is insignificant (ref. 2,8), and a clear explanation of the disruption phenomena remains to be established.

Unfortunately, thermophysical, thermochemical, and chemical kinetic properties for these alkanes are not very well defined (ref. 2). Experimental values of thermophysical parameters have been determined only at low temperatures, and theoretical evaluations based on ideal gas properties to guide extrapolations to flame temperatures are in significant disagreement (ref. 2). More importantly, the detailed kinetic mechanisms for large alkanes are only qualitatively understood (ref. 20). A 96 step semi-empirical mechanism has been proposed by Warnatz for predicting laminar pre-mixed flame propagation (ref. 21) for n-heptane-air flames, and this work has formed the basis for several studies on diffusion flames and reduced model development (refs. 4,22). The principal empiricism is the description of n-heptyl radical decomposition into the unlikely products of CH_3 + 2 C_3H_6 (in fixed ratio) rather than the expected mixture of β-scission products, C_2H_4, C_2H_5, C_3H_6, C_4H_8, CH_3, and C_3H_{10} (ref. 20), which are, in fact, evidenced in n-heptane-air diffusion flame structures (ref. 23) and flow reactors (ref. 24). More complex detailed kinetic mechanisms have been developed for autoignition studies in engines (up to 5000 reaction steps), but these mechanism involve considerable uncertainty and low and intermediate oxidation chemistry of little relevance in diffusion flames. However, as a means of developing ground- and space-based experimental test matrices, initial computations have been performed using the CRFM and two step semi-empirical kinetics with reversible CO/CO_2 chemistry (refs. 3,4,8). Numerical constants in the kinetic mechanism were adjusted to reproduce suspended droplet extinction diameter data (ref. 25) of n-heptane at low pressure (no soot formation), and calculations were performed to determine the burning characteristics of isolated n-heptane droplets under various ambient pressures, oxygen indices, diluents (nitrogen, helium), and initial diameters.

Figure 1 is typical of results from parametric calculations in which the ignition energy (magnitude) and (spatial) deposition parameters were varied for droplet burning in helium (refs. 3,4,8). The displayed function represents the minimum droplet size for which any amount of ignition energy specified would not produce ignition. At this droplet size, transport to the ambient and vaporization removed ignition energy from flammable regions at a rate more rapid than the chemical heat release rates anywhere surrounding the droplet region. As the critical ignition diameter increases, the amount of energy required to achieve ignition also increases. At the maximum critical ignition diameters displayed in the figures, no ignition energy could be found which would initiate droplet combustion. Experimentally, the critical ignition diameter must be large in comparison to the calculated extinction diameter. (Critical ignition energy predictions are unique to time-dependent computations.) Figure 2 displays calculated extinction diameter as a function of ambient pressure and oxygen index in helium diluent (refs. 3,4,8). Extinction diameter increases with decreasing pressure and with substitution of helium for nitrogen, i.e. by increasing the diffusivity relative to chemical kinetic conditions. Calculated results are similar to values (within 20%) from asymptotic analyses with 2-step (propene intermediate) reduced chemistry (see preceding paper, this workshop and refs. 3,4,8). Combined with the characteristic times required for various experimental procedures (e.g., droplet growth and deployment), and combustion properties (e.g. controlled sooting by selection of appropriate pressure, diluent, and oxygen indices) a test matrix envelope have been developed for proposing ground- and space-based microgravity experiments, e.g. Fig. 3 (Refs. 3,4,8).

As noted above, soot formation and accumulation effects are important factors in determining the burning characteristics of droplets. No theoretical model presently exists which explicitly includes sooting. Previous investigations have addressed the formation of the sootshell by balancing thermophoretic and viscous drag forces acting on a soot particle (refs. 26,17). However, the lack of detailed information regarding the distribution of the gas-phase transport and thermophysical properties prevented accurate determination of the sootshell position. Using the simplified chemistry for n-heptane described above (with no soot formation mechanism included) and temperature-dependent thermophysical properties, the CRFM model was used to estimate these parameters by calculating the transient gas-phase field distributions between the droplet surface and the flame location (ref. 8).

Once formed in the diffusion flame region, soot particles are acted upon by viscous drag (caused by Stefan flow), diffusion and thermophoresis, i.e. particle transport caused by a temperature gradient in the surrounding gas-phase (ref. 27). Because the sootshell location is much closer to the droplet surface than the flame and mass diffusion should be important only near the flame where the concentration gradients are large, this mode of particle transport can be neglected. Waldman and Schmidt (ref. 28) analyzed the viscous drag and thermophoretic force acting on a small spherical particle by calculating the momentum transferred per unit time to the particle by gas molecule collisions. The resulting force equation, solved at equilibrium, gives the thermophoretic flux, ρV_t, as

$$\rho V_t = \frac{-3\mu \frac{dT}{dr}}{4(1+\pi\alpha/8)T} = f(r) \qquad (Eqn.\ 1)$$

where ρ is the gas density, V_t is the relative velocity experienced by the particle, μ is the viscosity, and α is the thermal accommodation factor which is usually assigned a value of 0.9. Note that thermophoretic flux is independent of particle size for sizes on the order of incipient soot particles (ref. 29), i.e. for particles that are much smaller than the mean free path. For conditions under which soot agglomeration is prevalent, mean particle size may become much larger than the mean free path. The thermophoretic flux formulation is then defined as (ref. 27):

$$\rho V_t = \frac{-2\lambda^2 \sigma \rho \frac{dT}{dr}}{(2\lambda + \lambda_p)P} = f(r) \qquad (Eqn.\ 2)$$

where λ and λ_p are the thermal conductivities of the gas and the particle. The term, σ, is a dimensionless constant that relates the slip velocity at the particle surface and the gas-phase temperature gradient, usually assigned a value of 0.2. The thermal conductivity of soot particles was estimated from the temperature-dependent values for amorphous carbon (ref. 30).

When the surrounding gas-phase produces a Stefan flux, ρV, equal to ρV_t, the forces acting on the particle will be counter-balanced and the particles will accumulate to form the sootshell. Figure 4 displays the modeling results for the Stefan, the small-particle thermophoretic [denoted as SPT, Eqn. 1] and the large-particle thermophoretic [denoted as LPT, Eqn. 2] velocities, plotted versus normalized radius (divided by instantaneous droplet radius) for n-heptane burning in atmospheric pressure air. The time-dependence of mass gasification rate, droplet and flame dimensions and the temperature gradients will cause changes in these profiles. The results presented in Fig. 5 are typical of those produced under the quasi-steady burning conditions. The Stefan velocity near the droplet surface is observed to increase with radial position to a maximum near $r/r_o = 1.5$ and then decrease monotonically. Similar behavior is also observed for the SPT velocity, which matches the Stefan velocity at a normalized radius of 5.5. Considering that the calculated flame standoff ratio is 10 (in comparison to about 8 experimentally), this prediction is quite reasonable. The principal source of the disparity is that the calculated gasification rates are approximately 36% higher than the values measured for the most quiescent n-heptane droplet combustion experiments. Under sooting conditions, the portions of the gasified fuel which forms soot also possess negligible specific volume when compared to that of the gaseous species, which reduces the flame stand-off ratio. Scaling of the Stefan flux by the ratio of the experimental and calculated gasification rates and incorporating the flame contraction effects by reducing the distance between all calculated node locations by a factor of

$$F(t) = \frac{[\frac{d_{flame}}{d_{drop}}]_{(exp,\ t)}}{[\frac{d_{flame}}{d_{drop}}]_{(model,\ t)}}$$

calculations were performed for each droplet combustion time step to determine the location of the Stefan/thermophoretic flux equilibrium. The model-generated soot standoff ratios compare favorably with experimentally measured values (within 10%), see Fig. 5. Similar model calculations were also performed for droplet combustion in higher oxygen indices. For the 30%, 40% and 50% oxygen concentrations in nitrogen, the calculated soot standoff ratios were reduced to 2.65, 2.54 and 2.46, respectively (compared to measured ratios at 40% and 50% oxygen of approximately 2.2). Similar reductions for increasing oxygen indices have also been reported in ref. 31. For all oxygen concentrations, the calculated Stefan velocities were larger in magnitude than the minimum convective velocities required for equilibrium between viscous drag and LPT forces (within region bounded by droplet surface and flame front). This suggests that when larger soot agglomerates form, they should be transported towards the flame and eventually pass through it. This behavior was, in fact, observed in experiments at high oxygen/nitrogen ratios (> 0.4) for both n-decane and n-heptane fuel droplets.

It appears that thermophoretic effects are unlikely to lead to soot particle deposition on the liquid surface (speculated to lead to disruption) since viscous drag dominates very near the droplet surface. The flame would need to regress toward the droplet for a force imbalance to favor thermophoretic soot deposition. Regression of the flame through any part of the soot shell would expose the nascent soot particles to oxygen and lead to violent ignition processes in the gas phase surrounding the droplet. More refined analyses which explicitly include sooting effects will be needed to fully understand the mechanism(s) which result in reduced gasification rates and disruption. Areas of continuing interest also include the analysis of the internal circulation likely introduced by the experimental droplet deployment mechanism, and the small, but finite relative gas-droplet motions produced by all known techniques for droplet deployment and ignition. Improved experimental methods to characterize these attributes, and means to include their effects (as well as those of sooting) in the theoretical analyses, are presently being pursued.

Recently, we have incorporated the 96 step mechanism of Warnatz (ref. 21) in CRFM, along with multi-component transport to investigate unsteady burning behavior of n-heptane droplets, such as droplet heating before and after ignition, variation of the gasification rate and flame standoff ratio under limiting conditions of no droplet heating (infinitesimal heat capacity), conduction-limited heating, and infinite internal heat conduction (rapid liquid mixing). Time dependent calculations were performed for a 1 mm n-heptane droplet burning in ambient air. An initial vaporization period, followed by ignition by imposition of a spherically symmetric hot shell were studied. Initially, the no-droplet heating configuration was studied to investigate non-steady burning characteristics, and then more realistic liquid-phase heat transfer conditions were included. Species profiles are shown for quasi-steady burning in Fig. 6.

The model simulations suggest that the calculated flame stand-off ratio continuously increases even after the gasification rate reaches 99% of the quasi-steady value (for times $t/t_b > 0.1$, t_b = total burning time), see Fig 7. This unsteadiness has been previously suggested to be due to fuel vapor accumulation effects between the droplet surface and the flame (ref. 32). However, after t/tb> 0.1, the rate of fuel accumulation is near zero and eventually becomes negative due to droplet regression and flame contraction. The initial droplet heating period is strongly influenced by internal circulation. However, after initial transient period, the flame stand-off ratio, the gasification rate, the gas phase temperature and species profiles are not affected by the liquid phase heat transfer mechanism, even though the internal droplet temperature distribution may continue to change

(Fig. 8). Flame unsteadiness, is apparently also not related to internal droplet heating and appears to result primarily from a purely transient phenomenon associated with diffusion flame structural changes and the resulting changes in transport properties in the vicinity of the droplet. Further calculations to study the effects of the Warnatz mechanism on extinction diameter predictions are underway.

Future Work

In the near term, areas of theoretical interest include: improvement of the chemical models utilized for both computational and asymptotic approaches, improvement in understanding the effects of soot on droplet burning phenomena, and consideration of the low relative gas/droplet convection (which is inherent in droplet generation, deployment, and ignition), and assessing the effects of internal circulation induced by growth, deployment and ignition methods. Experimentally, additional efforts are underway to further reduce perturbations caused by droplet deployment and ignition methods, and to qualitatively image some of the flame species profiles, specifically, OH. Finally, the thermo-chemical and chemical kinetic foundations for n-heptane combustion need further improvement. As part of another study on autoignition chemistry of internal spark ignition fuels (e.g., see ref. 24), the author's laboratory is developing a homogenous kinetic experimental database on n-heptane oxidation which will be useful in improving and validating a more appropriate chemical mechanism for future use.

Acknowledgements

The work at Princeton was supported by NASA-LeRC of Cleveland, OH. under contract number #NAS3-1231. Contributors to this research include, Dr. S.Y. Cho, Dr. M. Y. Choi, Mr. P. Michniewicz., Mrs. Y. Stein, and Mr. J. Sivo. MYC was partially supported by the NASA Graduate Researcher Fellowship Program from 1988-1991.

References

1. Williams, F.A.: Diffusion Flames and Droplet Burning, Combustion Theory, 2nd Ed., Benjamin/Cummings Publ. Co., Menlo Park, CA, 1985, p. 52.
2. Choi, M.Y., Cho, S.Y. Dryer, F.L., and Haggard, J.B. Jr.: Some Further Observations on Droplet Combustion Characteristics: NASA LeRC-Princeton Results, AIAA/IKI Microgravity Science Symposium, AIAA Conference Proceedings (ISBN 1-56347-001-2), 1991, p. 294.
3. Choi, M.Y., Cho, S.Y., Dryer, and Haggard, J.B. Jr.: Computational/Experimental Basis for Conducting Alkane Droplet Combustion Experiments on Space-Based Platforms, IUTAM Symposium on Microgravity Fluid Mechanics, Bremmen, FRG, (Rath, H. J., ed.). Springer-Verlag, Berlin, 1992, p. 337.
4. Williams, F.A., Dryer, F.L.and Haggard, J.B. Jr.: Preliminary Science Requirements Document for the Droplet Combustion Apparatus, NASA-Lewis Research Center, November 1, 1991.
5. Cho, S.Y., Yetter, R.A. and Dryer, F.L.: Computer Model For Chemically Reacting Flow With Complex Chemistry/Multi-Component Molecular Diffusion/Heterogeneous Processes, Journal Of Computational Physics, 101, 1992. In press.
6. Cho, S.Y., Choi, M.Y. and Dryer, F.L.: The Extinction of a Free Methanol Droplet in Microgravity, Twenty-third Symposium (International) on Combustion, The Combustion Institute, 1990, p.1611.
7. Lee, A., Law, C.K. and Makino, A.: An Experimental Investigation on the Droplet Vaporization and Combustion of Alcohol Fuels, Fall Eastern Section Meeting of the Combustion Institute, Orlando, FL, 1990.
8. Choi, M.Y.: Droplet Combustion Characteristics under Microgravity and Normal Gravity Conditions, PhD Thesis, Dept. of Mechanical and Aerospace Engineering, Princeton University, Princeton, NJ, 1992, Report MAE T-1937.
9. Kee, R.J., Warnatz, J., and Miller, J.A.: TRANS, Sandia National Laboratories, Livermore, CA, 1983, Report No. 83-8209.
10. Norton, T.S. and Dryer, F.L.: Some Observations on Methanol Oxidation Chemistry, Comb. Sci. and Tech., 63, 1989, p.107.
11. Norton, T.S. and Dryer, F.L.: Toward a Comprehensive Mechanism for Methanol Pyrolysis, Int. J. Chem. Kin., 22, 1990, p. 219.
12. Egolfopoulos, F.N., Du, D.X., and Law, C.K.: A Comprehensive Study of Methanol Kinetics in Freely-Propagating and Burner-Stabilized Flames, Flow and Static Reactors, and Shock Tubes, Comb. Sci. and Tech., 83, 1992, p. 33.
13. Grotheer,, H,H,, Kelm, Driver, H.S.T., Hutcheon, R.J., Lockett, R.D., and Robertson, G.N.: Elementary Reactions in the Methanol Oxidation System. Part I: Establishment of the Mechanism and Modeling of Laminar Burning Velocities. Part II.: Measurement and Modeling of Autoignition in a Methanol-Fuelled Otto Engine, Berichte der Bunsengesellschaft, to appear in October, 1992 Issue.
14. Held, T.J.: PhD Thesis, Methanol, Iso-butene, and MBTE Oxidation in a Flow Reactor: the Effects of Ambient Pressure, Dept. of Mechanical and Aerospace Engineering, Princeton University, Princeton, NJ, 1992. In Preparation.
15. Law, C.K. and Williams, F.A.: Kinetics and Convection in the Combustion of Alkane Droplets, Comb. and Flame, 19, 1972, p. 393.
16. Choi M.Y., Dryer, F.L., Card, J.M., Williams, F.A., Haggard, J.B. Jr., and Borowski, B.A.: Microgravity Combustion of Isolated n-Decane and n-Heptane Droplets, AIAA Paper No. 92-242, January, 1992.
17. Shaw, B.D., Dryer, F.L., Williams, F.A. and Haggard, Jr., J.B.: Sooting And Disruption In Spherically-Symmetrical Combustion Of Decane In Air, Acta Astronautica, 17, 1988, p. 1195.
18. Choi, M.Y., Dryer, F.L. and Haggard, Jr., J.B.: Observation of a Slow-Burning Regime for Hydrocarbon Droplets: n-Heptane/Air Results, Twenty-Third Symposium (International) On Combustion, The Combustion Institute, 1990, pg. 1597.
19. Jackson, G.S. and Avedisian, C.T.: Possible Effects of Initial Diameter in Spherically Symmetric Droplet Combustion of Sooting Fuels, Fall Eastern States Technical Meeting, The Combustion Institute, Ithaca, NY, November, 1991.
20. Dryer, F.L.: The Phenomenology of Modeling Combustion Chemistry, Fossil Fuel Combustion (Bartok, W. and Sarofim, A, eds.), Wiley and Sons, NY, 1991.
21. Warnatz, J.: Chemistry of High Temperature Combustion of Alkanes up to Octane, Twentieth Symposium (International) on Combustion, The Combustion Institute, 1984, p. 845.
22. Bui-Pham, M. and Sheshadri, K.: Comparison Between Experimental Measurements and Numerical Calculations of the Structure of n-Heptane-air Diffusion Flames, Comb. Sci. and Tech., 79, 1991, p. 293.

23. Kent, J.H. and Williams, F.A.:Extinction of Laminar Diffusion Flames for Liquid Fuels, Fifteenth Symposium (International) on Combustion, The Combustion Institute, 1974, p. 315.
24. Kennedy, S, Brezinsky, K. and Dryer, F.: Flow Reactor Oxidation Studies of the Extent of Reaction in Heptane/Iso-octane Mixtures as a Function of Octane Number, Eastern Sectional Meeting of the Combustion Institute, Philadelphia, PA, 1985. Also Kennedy, S. BSE Thesis, Dept. of Chemical Engineering, Princeton University, Princeton, NJ, 1986.
25. Law, C.K. and Chung, S.H.: An Experimental Study of Droplet Extinction in the Absence of External Convection, Comb. and Flame, 64, 1986. p. 237.
26. Green, G.J., Dryer, F.L., and Sangiovanni, J.J.: Cenosphere Soot Agglomerates Formed During Low Reynolds Number Combustion Of Isolated Free Droplets, Paper presented at the 1984 Fall Eastern States Technical Meeting of the Combustion Institute, Gaithersburg, MD, 1984.
27 Friedlander, S.K.: Smoke, Dust and Haze, Wiley & Sons, NY, 1977.
28. Waldmann, L. and Schmitt, K.H.: Thermophoresis And Diffusiophoresis Of Aerosols, Aerosol Science, (Davies, C.N. ed.), Academic Press, NY, 1966, Chpt VI.
29. Palmer, H.B. and Cullis, H.F.: The Chemistry And Physics Of Carbon, Marcel Dekker. Vol. 1, 1965, p. 265.
30. Thermophysical Properties Of Matter, (Touloukian, Y.S. and Ho, C.Y. ,eds.), Plenum Press, NY, 1972.
31. Sangiovanni, J.J. and Liscinsky, D.S.: Soot Formation Characteristics of Well Defined Spray Flames, Twentieth Symposium (International) On Combustion, The Combustion Institute, Pittsburgh, 1984, p. 1963.
32. Law , C.K., Chung, S.H., and Srinivasan, N.: Gas Phase Quasi-Steadiness and Fuel Vapor Accumulation Effects in Droplet Burning, Comb. and Flame, 38, 1980, p. 173.

Figures

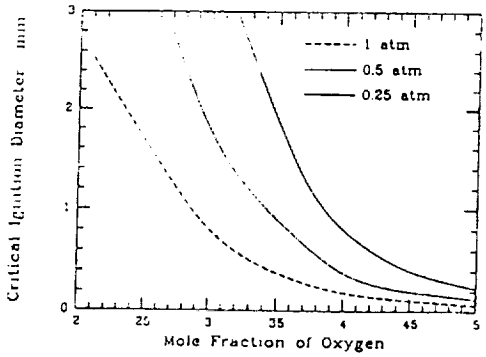

Figure 1. Computed Critical Ignition Diameters for n-Heptane Burning in Oxygen/Helium. (refs. 3,4,8).

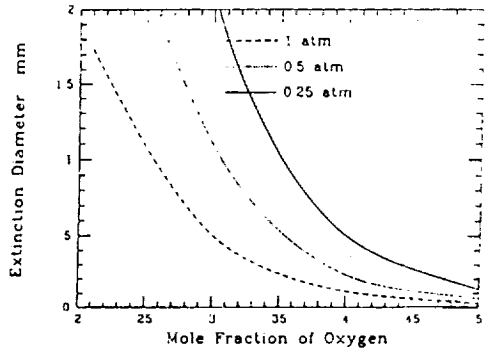

Figure 2. Computed Extinction Diameters for n-Heptane Burning in Helium Diluent. (refs. 3,4,8).

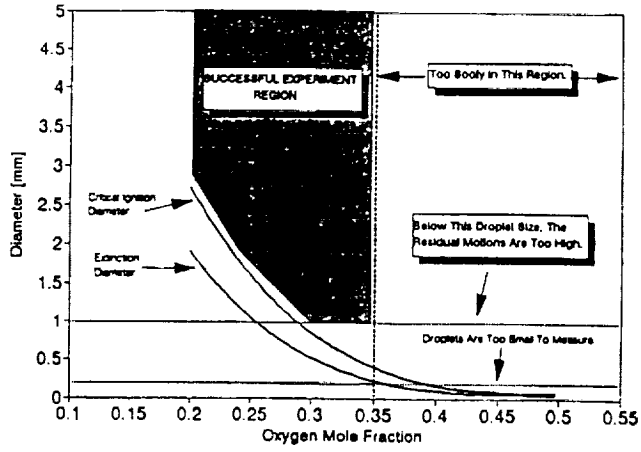

Figure 3. Test Envelope for n-Heptane Droplet Studies in Droptowers and on Space-based Platforms in Helium Diluent. (refs 3,4,8).

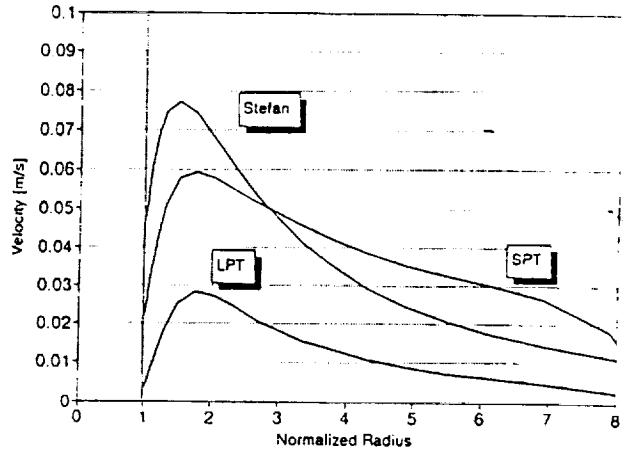

Figure 4. Predicted Stefan, Small Particle Thermophoretic (SPT), and Large Particle Thermophoretic (LPT) Velocity Distributions at Quasi-Steady Conditions for n-Heptane-Air (Nitrogen) Droplet Burning (1 atm.).

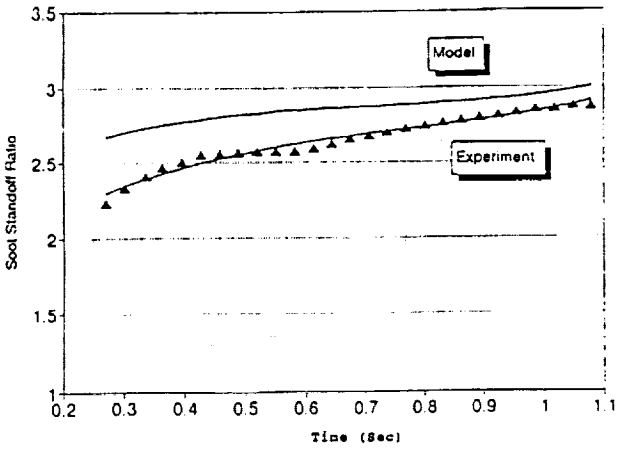

Figure 5. Predicted /Experimental Sootshell Stand-off Ratio for n-Heptane-Air (Nitrogen) Droplet Burning (1 atm.).

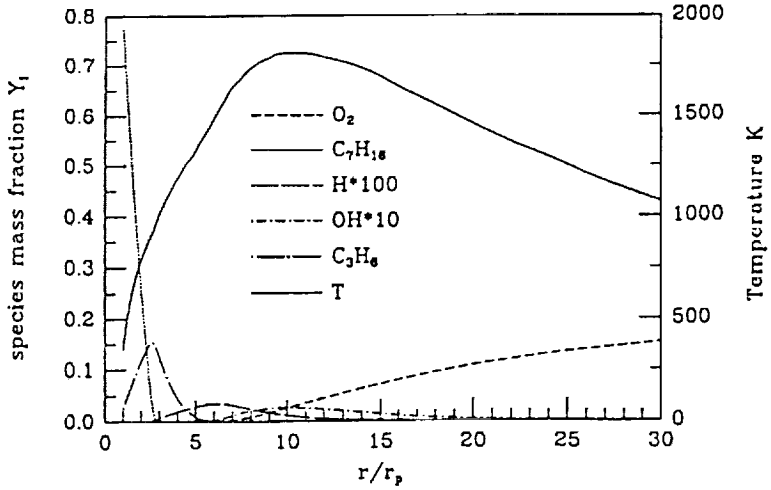

Figure 6. Predicted Species Profiles for Quasi-Steady n-Heptane-Air Droplet Burning (1 atm.) using the Detailed Mechanism of Warnatz (21). No Droplet Heating.

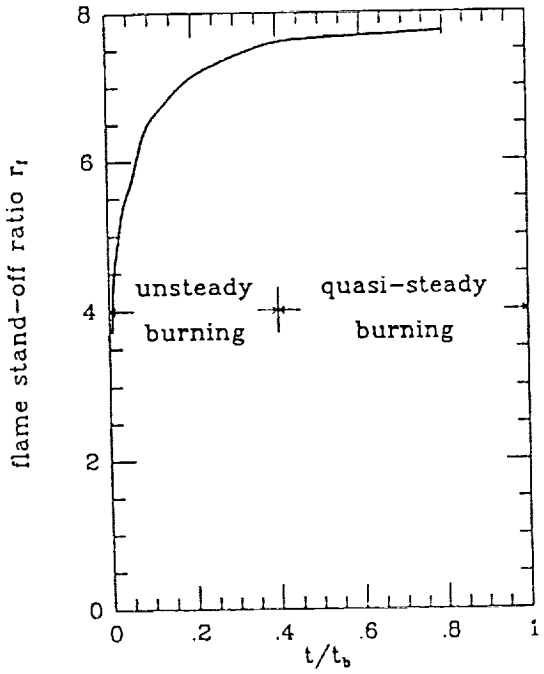

Figure 7. Calculated Flame Stand-off Ratio for n-Heptane-Air Droplet Burning with Mechanism of Warnatz (21). No Droplet Heating.

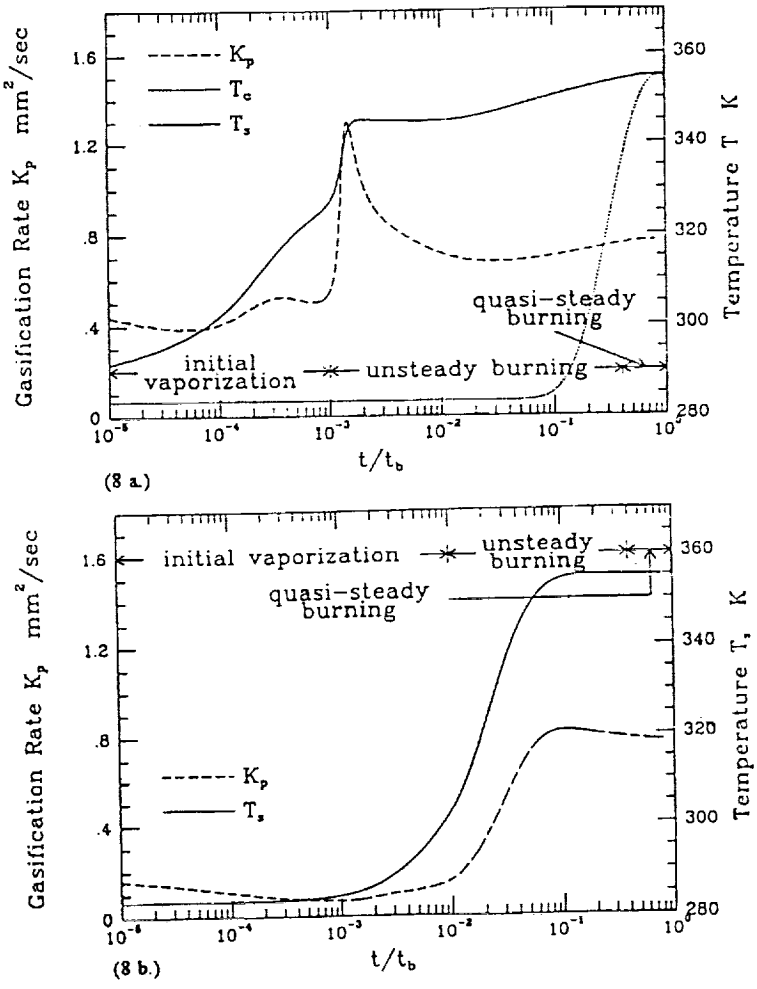

Figure 8. The Temporal Variation of Gasification Rates (K_p), Droplet Surface Temperature (T_s) and Droplet Center Temperature (T_c). (a). Conduction Limit Model. (b). Infinite Heat Conductivity Model ($T_s = T_c$).